Selecte growth of large chiral angle single-walled carbon nanotubes

11 AUTHORS, INCLUDING:

Thierry Michel
Université de Montpellier
36 PUBLICATIONS   639 CITATIONS

SEE PROFILE

Vincent Jourdain
Université de Montpellier
41 PUBLICATIONS   580 CITATIONS

SEE PROFILE

Jean-Louis Sauvajol
Université de Montpellier
293 PUBLICATIONS   4,972 CITATIONS

SEE PROFILE

Bruno Chaudret
French National Centre for Scientific Resea…
278 PUBLICATIONS   9,253 CITATIONS

SEE PROFILE

Selective growth of large chiral angle single-walled carbon nanotubes

Matthieu Paillet [a,*,1], Jannik C. Meyer [b,1], Thierry Michel [a], Vincent Jourdain [a],
Philippe Poncharal [a], Jean-Louis Sauvajol [a], Nadège Cordente [c], Catherine Amiens [c],
Bruno Chaudret [c], Siegmar Roth [b], Ahmed Zahab [a]

[a] Laboratoire des Colloïdes, Verres et Nanomatériaux U.M.R. CNRS 5587,CC 026-Université Montpellier II, 34095 Montpellier cedex 5, France
[b] Max-Planck Institut für Festkörperforschung, Heisenbergstrasse 1, 70569 Stuttgart, Germany
[c] Laboratoire de Chimie de Coordination du CNRS, 205, route de Narbonne, 31077 Toulouse cedex, France

Abstract

We have developed a versatile catalyst-assisted chemical vapor deposition (CVD) technique for the synthesis of single-walled carbon nanotubes (SWNTs) from discrete nickel nanoparticles (average diameter of 4.7 ± 1.5 nm). Atomic force microscopy (AFM), transmission electron microscopy (TEM) and electron diffraction are used to characterize these as-grown nanotubes. On a particular sample we found that the SWNTs have an average chiral angle of 25.3°. This result shows that a control of the chiral angle of SWNT with large diameters (mean diameter = 1.75 nm) and with a relatively broad diameter distribution (standard deviation = 0.5 nm) is achievable to a certain extent.
© 2006 Elsevier B.V. All rights reserved.

Keywords: Nanotubes; Chemical vapor deposition; High resolutions electron microscopy; Electron diffraction

1. Introduction

Single-walled carbon nanotubes (SWNTs) have served as prototype system to study low-dimension physics. Since the properties of SWNTs in general strongly depend on their structural characteristics (mainly the diameter d and chiral angle θ), the control and characterization of these parameters is of major interest when studying their physical properties [1] and an important step towards electronic and optical applications of SWNTs. The atomic structure of a given nanotube can be defined either by the couple d and θ or by two integers, i.e. its structural indices n and m [2]. The experimental determination of the (n, m) indices and their distribution in SWNT samples appears as an important achievement both for the control of SWNT atomic structure and for an extensive understanding of their growth mechanism.

The use of fluorescence spectroscopy allowed recently the characterization of the (n, m) distribution of bulk samples synthesized by chemical vapor deposition [3,4]. Small diameter SWNTs (i.e. <1 nm) were found to have a preferential near-armchair lattice orientation (i.e. θ close to 30° or m close to n).

In this report, the (n, m) distribution of SWNTs synthesized by supported catalyst chemical vapor deposition is achieved by electron diffraction. This characterization technique includes metallic nanotubes contrary to fluorescence spectroscopy. Moreover, our sample preparation method allows to study low-density individual SWNT samples. On a particular SWNT sample we found that the SWNT population is enriched in armchair and close to armchair nanotubes even if their average diameter is relatively large and their diameter distribution relatively broad.

2. Experimental section

Nickel nanoparticles (NP) preparation has been reported in detail elsewhere [5]. The nanoparticles were dispersed in ethanol and deposited on a 4×4 cm^2 silicon substrate with a 200 nm thermally grown oxide layer by spin coating (30 Hz for 1 min). The nanoparticle (NP) size distribution before synthesis was estimated to 4.7 ± 1.5 nm from their heights

measured on AFM topographic images. The average NP density is 20 NP/μm².

Nanotube growth on the substrate took place in a 3″ quartz tube reactor at 900 °C for 10 min under combined flows of 1200 sccm CH_4/600 sccm H_2 (purities of 99.95% and 99.995% resp.). Before the synthesis temperature is reached, the substrates are first heated in air up to 650 °C, and then the reactor is purged under an argon (purity of 99.99%) flow (5000 sccm) for 15 min.

Carbon nanotubes were characterized by atomic force microscopy (AFM) (Dimension 3100, Nanoscope IIIa, Digital Instruments) operating in the tapping mode with commercial Si cantilevers (spring constant ~35 N/m) and integrated tips.

A recently developed technique [6–8] was used to observe nanotubes, which were grown on the substrate, by High Resolution Transmission Electron Microscopy (HR-TEM) (Philips CM200, 120 kV) and electron diffraction (recorded on image plates in a Zeiss 912 Ω microscope operated at 60 kV). Shortly, a metallic structure is created after growth on top of the nanotubes by e-beam lithography. Next, the substrate is cleaved close to this structure. Then, it is etched in such a way that a part of the structure is reaching out over the edge of the substrate. This freestanding structure allows TEM imaging of freely suspended carbon nanotubes sticking to the metal pads.

3. Results and discussion

Fig. 1a and b show typical AFM images of nanotubes grown at 900 °C using methane as carbon source. The average length of the SWNTs is superior to 1 μm and their average density is ≈0.2/μm². As revealed by HRTEM (Fig. 1c–e), the nanotubes are single-walled with a well-defined wall structure and mainly individual with few amorphous carbon residues. The mean diameter of the SWNTs is 1.75 nm (±0.5 nm) from measurements on AFM topographic images (Fig. 2). Investigations of 7 different 100×100 μm² areas of the 4×4 cm² substrate by AFM revealed that the SWNT diameter and length distributions are homogenous over the whole sample. The density of SWNTs however was found to fluctuate slightly between 0.05 to 0.5 SWNTs per square micron. These fluctuations are consistent with those of the NP density.
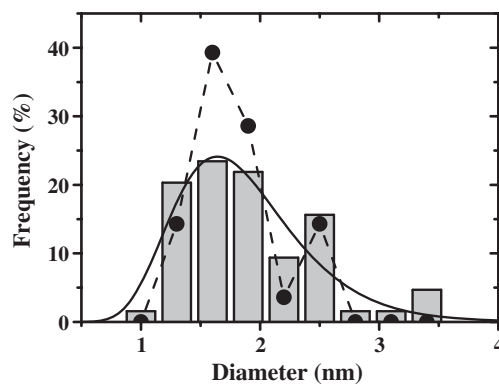
Fig. 2. Histogram of ≈100 individual nanotube diameters measured by AFM. The solid circles linked with the dashed line correspond to the diameter statistic of the 28 SWNTs investigated by electron diffraction. The solid line corresponds to a lognormal fit of the AFM data.

As reported for experiments carried out with ethylene [9–11], the nanotube diameter distribution shows a heavy mismatch with the nickel NP size. This point is not the purpose of this article and is discussed in details elsewhere [9,11]. In our previous work [9], we have reported that both SWNTs and Multiwalled carbon nanotubes (MWNT) were grown when methane was used instead of ethylene. This former result was accompanied with changes in the NP size distribution measured after synthesis. Further investigations bring us to the conclusion that NP aggregation was responsible for the MWNT growth. When aggregation is avoided the selective growth of 1.75±0.5 nm SWNTs is fully reproducible.

The very straight and well-separated nanotubes obtained by our sample preparation method allow a reliable analysis by electron diffraction. The experimentally obtained diffraction pattern is compared with simulated diffraction patterns, and the nanotube indices and the incidence angle of the simulation are adjusted until the simulated pattern matches the experimental one. We verify that only exactly one pair of indices (n, m) matches the experimental pattern, by checking that the simulated patterns for all nearby indices clearly deviate from the experimental one for any incidence angle. Details of our diffraction analysis procedure are given in Ref. [7]. Examples of experimental and simulated patterns of a (10,10) and a (20,16)
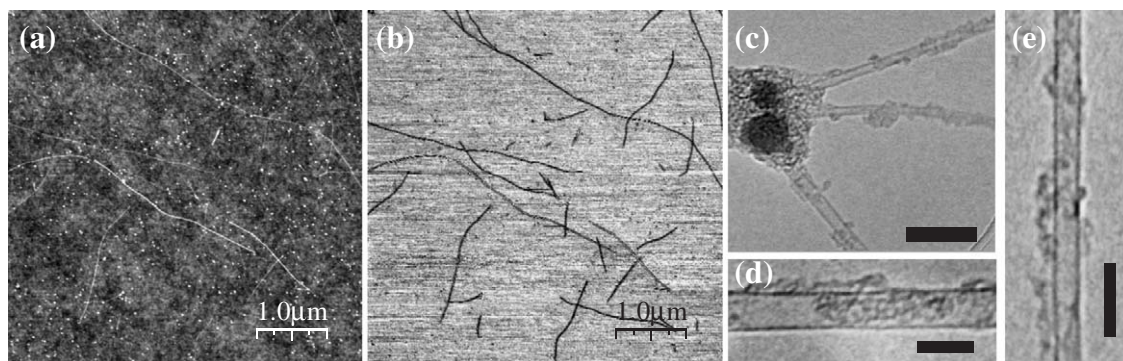
Fig. 1. (a) and (b) AFM images of nanotubes grown from Ni nanoparticles (NP) on silicon substrates with a 200 nm thermally grown oxide layer at 900 °C for 10 min using 1200 sccm of CH4: (a) topography, (b) phase. (c)–(e) HRTEM images of the same sample. Scale bars are: (c) 10 nm, (d) and (e) 5 nm. The SWNT diameters are: (c) 1.15, 1.2 and 1.75 nm, (d) 3.2 nm and (e) 1.6 nm. Most of the amorphous carbon are deposited during the HRTEM analysis.

nanotubes synthesized by the CVD method described here are presented on Fig. 3(a) and (b), respectively.

Our method allows to perform a statistical analysis of the (n, m) distribution in CVD grown individual SWNTs. A complete list of 28 isolated SWNTs examined randomly is given in Fig. 3 (c). The diameter distribution of these 28 SWNTs incoming from different pieces of our $4 \times 4 \text{ cm}^2$ sample is shown on Fig. 2. The good agreement with the diameter distribution obtained by AFM on a larger number of tubes allows to conclude that the electron diffraction data is representative of the global sample.

Fig. 4(a) shows the statistics of chiral angles obtained from nanotubes all grown in the same CVD process. The electron diffraction analysis gives more precise information than AFM or TEM images and clearly shows that the rolling angle is not randomly distributed, but is grouped towards the armchair orientation. From a global point of view, the mean angle is 25° (standard deviation ∼6°) but 2/3 of the SWNTs investigated have chiral angles superior to this value. For comparison a simple count of the possible structures within the diameter range of 1.75 ± 0.5 nm, leads to an average chiral angle of 14.7° with a repartition more or less homogeneous on all possible chiral angles (see Fig. 4). Looking at the electrical properties (deduced from the indices), we found in our sample 68% of semiconducting SWNTs, 11% of small gap semiconducting (semi-metallic) SWNTs and 21% of metallic (armchair) SWNTs. The semiconducting SWNT content is close to the theoretical value of ≈65%, but the amount of small gap semiconducting SWNTs is clearly decreased (≈31% is expected) and the number of armchair SWNTs is 5 times higher than the theoretically predicted amount (i.e. ≈4%).

Other samples prepared in the same experimental conditions show the same diameter distribution as presented on Fig. 2, their investigation by electron diffraction is in progress in order to confirm the reproducibility of the trend obtained here.

Electron diffraction is a direct measurement of the SWNT structural indices (n, m) and it includes metallic nanotubes. Some fluorescence spectroscopic results [3,4] show a similar trend, but are limited to semiconducting tubes and biased by a structure-dependent fluorescence quantum yield. The Raman study in Ref. [12] finds a more or less random distribution of
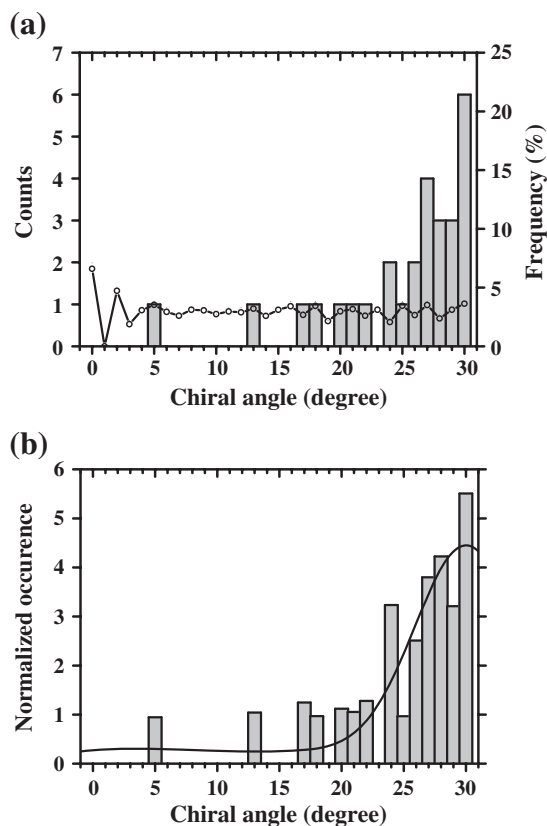

(a)

(b)

Fig. 4. (a) Histogram of the chiral angle distribution derived from the electron diffraction patterns of 28 individual SWNTs. The open circles linked by the solid line corresponds to the statistical distribution expected for SWNTs with diameters of 1.75 ± 0.5 nm (The different statistical weights of each nanotube are taken into account according to the diameter distribution displayed on Fig. 2). (b) Histogram showing normalized occurrence (normalized by dividing the observed number of nanotubes by the statistical number of nanotube species expected theoretically for each chiral angle) of characterized individual nanotubes versus chiral angle. Nanotubes of chiral angles >24° are strongly favored. The solid line corresponds to a Gaussian fit.

nanotube indices in HiPCO nanotubes. A recent extensive electron diffraction study also showed a rather uniform distribution for a carbon nanotube sample produced by arc discharge [13]. Note that all these index distributions are

(a) **(b)** **(c)**

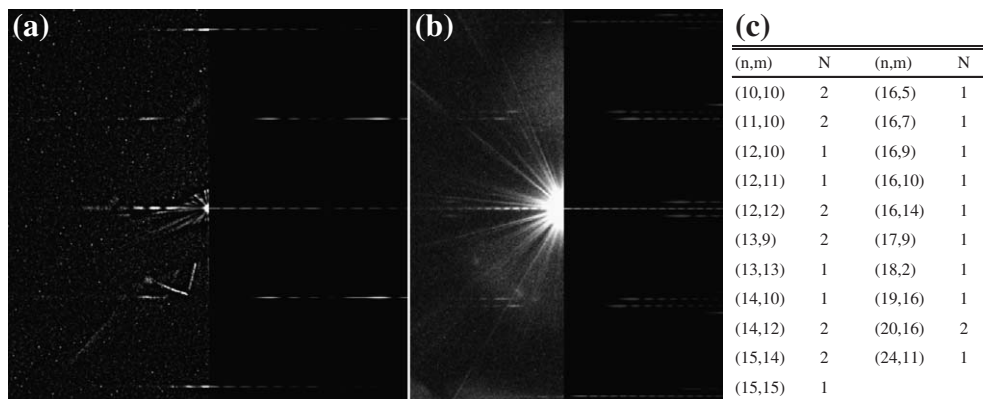| (n,m)	N	(n,m)	N
(10,10)	2	(16,5)	1
(11,10)	2	(16,7)	1
(12,10)	1	(16,9)	1
(12,11)	1	(16,10)	1
(12,12)	2	(16,14)	1
(13,9)	2	(17,9)	1
(13,13)	1	(18,2)	1
(14,10)	1	(19,16)	1
(14,12)	2	(20,16)	2
(15,14)	2	(24,11)	1
(15,15)	1		

Fig. 3. (a) and (b) Diffraction patterns of individual nanotubes: (a) a (10,10) and (b) a (20,16). On each image the left half is the experimental pattern and the right half is the corresponding simulated pattern. (c) List of the (n, m) indices of the 28 examined nanotubes with the number (N) of encounters of the corresponding nanotube species.

obtained from nanotubes grown with different methods and parameters. We can compare the angular selectivity in our material with the fluorescence studies of nanotubes produced by alcohol catalytic CVD (ACCVD) under optimized conditions [4] and grown from solid-supported Mo/Co catalyst (MoCo) [3]. An angle of 30° represents armchair nanotubes, 0° a zigzag tube, and an average of 15° is expected for a random distribution. The average angle in the MoCo material, calculated from the fractional intensities listed in Ref. [3], is 22.8°. The intensities in Ref. [4] are given only in a graphical representation, from which we estimate an average angle of ≈23°. We should however notice that the relative abundances are derived in Refs. [3] and [4] under the assumption of a structure independent fluorescence yield and that it was shown recently that fluorescence intensities are strongly affected by the nanotube chirality [14] (this is also the case for Raman scattering intensities [15]). In our sample the mean angle is 25° if we include all nanotubes, and 24° if we exclude the metallic tubes for a better comparison with the fluorescence spectroscopic results. Due to the much larger diameters obtained in our CVD process, there are many more different nanotube species possible within a given angle interval (e.g. ≈180 SWNTs for $1.25 \, nm \leq d \leq 2.25 \, nm$, 70 SWNTs for $1.2 \, nm \leq d \leq 1.65 \, nm$ [13] and ≈40 SWNTs for $0.6 \, nm \leq d \leq 1.05 \, nm$ [4]). The angular selectivity towards armchair tubes, however, is at least similar to the samples in Ref. [3] or [4]. This result shows that a control of the chiral angle of SWNT with large diameters and with a relatively broad diameter distribution is achievable to a certain extent.

As demonstrated in Ref. [4] the index distribution strongly depends on the growth conditions. The systematic study of different synthesis parameters on the (*n*, *m*) distribution presented in Ref. [4] demonstrated that the near-armchair chirality distribution is primarily due to smaller diameters. Such arguments can obviously not be used in our case. Preliminary studies on other samples of similar diameter distribution and grown by using ethylene at 850 °C showed no tendency for a particular chiral angle. This seems to support the idea that the carbon source plays an important role. Further investigations of the (*n*, *m*) distribution of different SWNT samples remain needed for an extensive comprehension of the SWNT growth mechanism and a specific understanding of the particular result presented here.

4. Conclusions

We have grown from discrete catalyst nickel nanoparticles by CVD high-quality isolated single-walled carbon nanotubes. Their diameter (1.75 ± 0.5 nm) and length (>1 μm in average) are homogenous on the whole substrate. An electron diffraction analysis carried out randomly over different pieces of this sample shows that the synthesis conditions used lead to the preferential growth of armchair and close to armchair SWNTs. This trend is similar to those found by fluorescence spectroscopy on small diameter SWNTs [3,4]. However, electron diffraction provides a direct measurement of the nanotube structure not influenced by optical absorption matrix elements, and it includes metallic nanotubes. Our result also shows that a control of the SWNT chiral angle can be achieved independently of a strict control of the SWNT diameter. Furthermore, preliminary results obtained on SWNTs synthesized with ethylene indicate that the carbon source plays an important role.

A precise characterization of the (*n*, *m*) distribution of SWNT samples, as presented here, is an important step towards the comprehension of SWNT growth mechanism and the challenging control of SWNT chirality. Systematic studies of the effects of the different synthesis parameters (temperature, carbon source, gas flows...) are in progress.

Acknowledgments

References

[1] H. Dai, J. Acc. Chem. Res. 35 (2002) 1035 (and references therein).
[2] N. Hamada, S. Sawada, A. Oshiyama, Phys. Rev. Lett. 68 (1992) 1579.
[3] S.M. Bachilo, L. Balzano, J.E. Herrera, F. Pompeo, D.E. Resasco, R.B. Weisman, J. Am. Chem. Soc. 125 (2003) 11186.
[4] Y. Miyauchi, S. Chiashi, Y. Murakami, Y. Hayashida, S. Maruyama, Chem. Phys. Lett. 387 (2004) 198.
[5] T. Ould Ely, C. Amiens, B. Chaudret, E. Snoeck, M. Verelst, M. Respaud, J.-M. Broto, Chem. Mater. 11 (1999) 526.
[6] J.C. Meyer, D. Obergfell, S. Yang, S. Yang, S. Roth, Appl. Phys. Lett. 85 (2004) 2911.
[7] J.C. Meyer, M. Paillet, G.S. Duesberg, S. Roth, Ultramicroscopy 106 (2006) 176.
[8] J.C. Meyer, M. Paillet, T. Michel, A. Moreac, A. Neumann, G.S. Duesberg, S. Roth, J.-L. Sauvajol, Phys. Rev. Lett. 95 (2005) 217401.
[9] M. Paillet, V. Jourdain, P. Poncharal, J.-L. Sauvajol, A. Zahab, J.C. Meyer, S. Roth, N. Cordente, C. Amiens, B. Chaudret, J. Phys. Chem., B 108 (2004) 17112.
[10] M. Paillet, V. Jourdain, P. Poncharal, J.-L. Sauvajol, A. Zahab, J.C. Meyer, S. Roth, N. Cordente, C. Amiens, B. Chaudret, Diamond Relat. Mater. 14 (9) (2005) 1426.
[11] M. Paillet et al., in preparation.
[12] H. Telg, J. Maultzsch, S. Reich, F. Hennrich, C. Thomsen, Phys. Rev. Lett. 93 (2004) 177401.
[13] Z. Liu, Q. Zhang, L.-C. Qin, Phys. Rev., B 71 (2005) 245413.
[14] S. Reich, C. Thomsen, J. Robertson, Phys. Rev. Lett. 95 (2005) 077402.
[15] M. Machon, S. Reich, H. Telg, J. Maultzsch, P. Oderjon, C. Thomsen, Phys. Rev., B 71 (2005) 035416.